Available online at www.sciencedirect.com
SCIENCE DIRECT®
Materials Science in Semiconductor Processing 8 (2005) 103–109
MATERIALS SCIENCE IN SEMICONDUCTOR PROCESSING

# Suppression of boron transient enhanced diffusion in silicon and silicon germanium by fluorine implantation

H.A.W. El Mubarek[a,*], Y. Wang[b], R. Price[c], J.M. Bonar[a], J. Zhang[c], P.L.F. Hemment[b], P. Ashburn[a]

[a]*School of Electronics & Computer Science, University of Southampton, Southampton, S017 1BJ, UK*
[b]*School of Electrical & Electronic Engineering, University of Surrey, Guildford, GU2 5XH UK*
[c]*Department of Physics, Imperial College, University of London, London, SW7 2AZ UK*

Available online 28 October 2004

**Abstract**

In this paper, a study is made of the effect of fluorine implantation on boron transient enhanced diffusion in Si and SiGe by characterising the diffusion of boron marker layers in Si and SiGe in samples with and without a 288 keV, $6 \times 10^{13}\,cm^{-2}$ $P^+$ implant and with and without a 185 keV, $2.3 \times 10^{15}\,cm^{-2}$ $F^+$ implant. It is shown that fluorine implantation totally eliminates boron transient enhanced diffusion caused by the phosphorus implant as well as significantly reduces boron thermal diffusion in both Si and SiGe. Fluorine SIMS profiles for both Si and SiGe samples show the presence of a shallow peak in the vicinity of the boron marker layer and a deep peak close to the range of the fluorine implant. Cross-sectional transmission electron micrographs show the presence of a band of dislocation loops that correlates with the position of the deep fluorine peak, but no defects are present in the position of the shallow fluorine peak. It is proposed that the shallow fluorine peak is due to vacancy-fluorine clusters that are too small to resolve by TEM. The role of the vacancy-fluorine clusters and the dislocation loops on the suppression of boron diffusion in Si and SiGe is discussed.
© 2004 Elsevier Ltd. All rights reserved.

*Keywords:* Boron; Diffusion; Silicon; Silicon germanium

## 1. Introduction

Over the past few years there has been considerable interest in the effect of fluorine on boron diffusion in silicon [1–18]. This research has been motivated by the requirement in advanced CMOS technologies to minimise boron diffusion for the formation of shallow source/drain junctions and sharply defined halo profiles [19,20]. The minimisation of boron diffusion is also important in bipolar transistors, where boron diffusion limits the achievable base width and hence the value of cut-off frequency that can be obtained [21]. The suppression of boron diffusion is difficult to achieve in practice because of both boron thermal diffusion and boron transient enhanced diffusion due to damage created in ion implantation [22].

Work on the effects of fluorine from a $BF_2^+$ implant showed that shallower junctions could be obtained when $BF_2^+$ was implanted instead of $B^+$ [1,7,8]. In later work [2–6,9–15,17,18] fluorine was implanted separately to the boron to characterise the effect of the fluorine on transient enhanced boron diffusion. This work showed that the fluorine implant reduced boron transient

*Corresponding author. Tel.: +44 2380 593737; fax: +44 2380 593029.
*E-mail address:* hawem@ecs.soton.ac.uk (H.A.W. El Mubarek).

1369-8001/$ - see front matter © 2004 Elsevier Ltd. All rights reserved.
doi:10.1016/j.mssp.2004.09.112

enhanced diffusion [2–5,9,11,13,14,16–18] and increased boron activity [2]. However, there have also been contradictory reports in the literature, which showed that fluorine implants had little or no effect on boron transient enhanced diffusion [10] and that fluorine enhanced boron diffusion in pre-amorphised silicon [15]. However, the mechanisms by which fluorine suppresses boron transient enhanced diffusion in silicon are poorly understood and there have been no reports of the effects of fluorine on boron diffusion in silicon germanium.

In this paper, a comparison is made of the effects of fluorine implantation on boron transient enhanced diffusion in silicon and silicon germanium. Boron SIMS profiles before and after anneal are studied in samples with and without a phosphorus selective implanted collector and with and without fluorine implantation. Fluorine SIMS profiles before and after anneal are also studied. Cross-sectional transmission electron microscope micrographs are presented for fluorine implanted samples and are used together with the fluorine SIMS profiles to interpret the mechanisms by which fluorine suppresses boron transient enhanced diffusion in Si and SiGe.

## 2. Experimental procedure

Low-pressure chemical vapour deposition at 800 °C was used to grow a Si starter layer, a 39 nm $Si_{0.89}Ge_{0.11}$ layer and a Si cap layer on (1 0 0) silicon wafers. A boron-doped marker layer was incorporated within the SiGe layer with a peak concentration of $1.2 \times 10^{19}\,cm^{-3}$. Molecular beam epitaxy at 520 °C was used to grow a silicon layer containing a buried boron-doped marker layer. Schematics of the epitaxial layers are shown in Fig. 1. Three types of samples were then produced from each wafer; the first had no implants (unimplanted), the second a phosphorus implant only ($P^+$ implanted) and the third a phosphorus and a fluorine implant ($P^+$ and $F^+$ implanted). A 288 keV, $6 \times 10^{13}\,cm^{-2}$ phosphorus implant was used with an energy and dose similar to those used for selective implanted collectors in bipolar and BICOMS technologies [23]. The $F^+$ was implanted at 185 KeV, $2.3 \times 10^{15}\,cm^{-2}$, with the energy chosen to give a fluorine peak coincident with the phosphorus peak. The samples were annealed by rapid thermal annealing in nitrogen at 1000 °C for 30 s. Boron (B11), fluorine (F19) and germanium (Ge 74) concentration depth profiles were obtained on all samples by secondary ion mass spectroscopy (SIMS). The layers were also analysed by transmission electron microscopy (TEM).

## 3. Results

Fig. 2(a) shows the effect of a $P^+$ implant on the boron diffusion in silicon in the absence of a $F^+$ implant. It can be seen that the $P^+$ implant causes significant extra diffusion of the boron marker layer compared with the unimplanted control sample. Comparing the boron profiles at a concentration of $1 \times 10^{17}\,cm^{-3}$, we find that the width of the $P^+$ implanted boron profile is 138 nm, compared with 108 nm for the unimplanted boron profile and 48 nm for the as-grown boron profile. These results indicate that the phosphorus implant is giving rise to transient enhanced diffusion of boron.

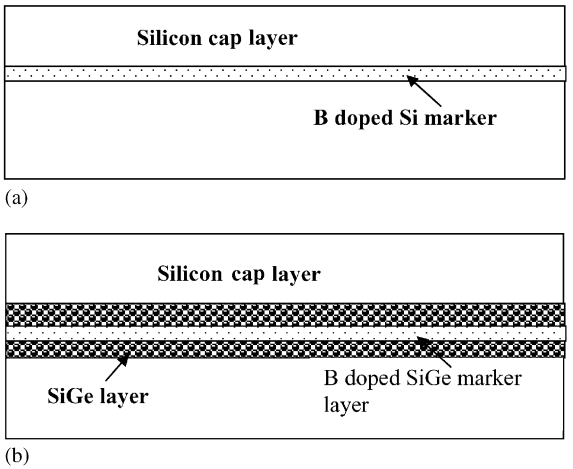
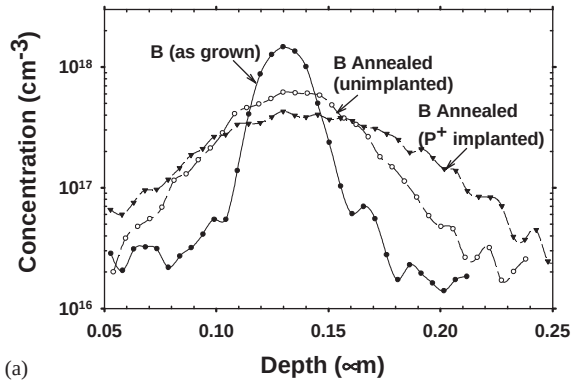



Fig. 1. A schematic of (a) silicon and (b) silicon germanium epitaxial layers.

Fig. 2(b) shows the effect of a $P^+$ implant on the boron diffusion in silicon germanium in the absence of a $F^+$ implant. It can be seen that the $P^+$ implant causes significant extra diffusion of the boron marker layer compared with the unimplanted control sample. In the sample implanted with $P^+$ only, the anneal significantly decreases the peak boron concentration in the SiGe layer from $1.2 \times 10^{19}$ to $3.2 \times 10^{18}\,cm^{-3}$ and gives considerable out-diffusion of the boron profile into the adjacent silicon layers. In contrast for the unimplanted sample, the decrease in the peak boron concentration in the SiGe layer is less, from $1.2 \times 10^{19}$ to $4.7 \times 10^{18}\,cm^{-3}$, and the out-diffusion of the boron profile into the adjacent silicon is also less. Comparing the boron profiles at a concentration of $1 \times 10^{17}\,cm^{-3}$, we find that the boron out-diffusion into the substrate of the $P^+$ implanted sample (62 nm) is 26 nm more than that of the unimplanted sample (36 nm). This translates to an enhancement factor of 72% in boron diffusion due to the phosphorus implant. This indicates that the phosphorus implant is giving rise to transient enhanced diffusion of boron in both SiGe and Si.

Fig. 3(a) shows the effect of a $F^+$ implant on boron transient enhanced diffusion in silicon samples implanted with $P^+$. The boron profile of the control unimplanted sample is also shown for comparison. It is



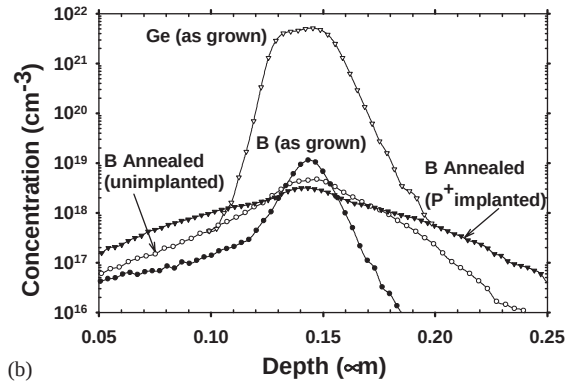
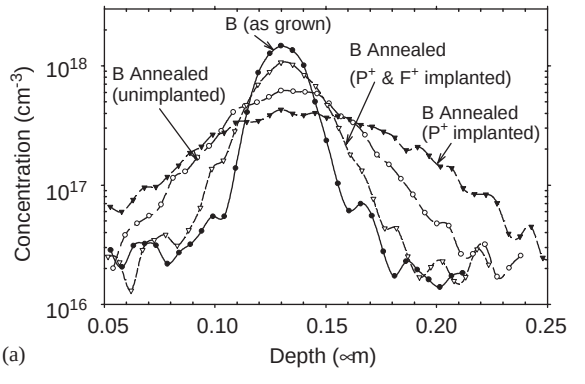




Fig. 2. Boron SIMS profiles in $P^+$ implanted and unimplanted samples after an anneal of 30 s at 1000 °C in dry $N_2$. As-grown boron and germanium profiles are also included for reference. Results are shown for (a) a silicon sample and (b) a silicon germanium sample.



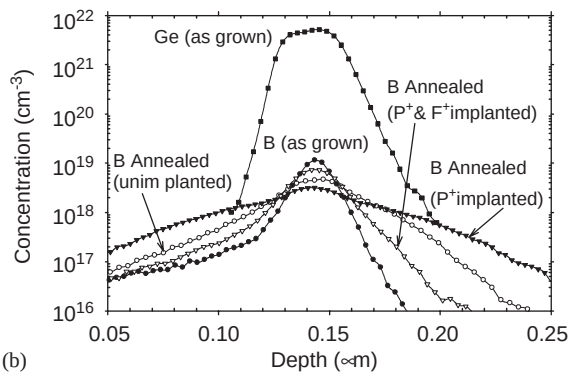




Fig. 3. Boron SIMS profiles in $P^+$ implanted, $P^+$ and $F^+$ implanted and unimplanted samples after an anneal of 30 s at 1000 °C in dry $N_2$. As-grown boron and germanium profiles are also included for reference. Results are shown for (a) a silicon sample and (b) a silicon germanium sample.

clear that there is dramatically less boron diffusion in the sample implanted with $F^+$. Comparing the boron profiles at a concentration of $1 \times 10^{17}\,cm^{-3}$, we observe that the diffusion of boron into the substrate in the $P^+$ and $F^+$ implanted sample (14 nm) is 42 nm less than that in the $P^+$ implanted sample (56 nm), and 17 nm less than that of the unimplanted sample (31 nm). This indicates that the $F^+$ implant has not only totally suppressed the boron transient enhanced diffusion caused by the $P^+$ implant but has also greatly reduced the thermal diffusion by a factor of 55%.

Fig. 3(b) shows the effect of a $F^+$ implant on boron transient enhanced diffusion in silicon germanium samples implanted with $P^+$. The boron profile of the control unimplanted sample is also shown for comparison. In the sample implanted with $P^+$ only, the anneal significantly decreases the peak boron concentration in the SiGe layer from $1.2 \times 10^{19}$ to $3.2 \times 10^{18}\,cm^{-3}$ and gives considerable out-diffusion of the boron profile into the adjacent silicon layers. In contrast, in the sample implanted with both $P^+$ and $F^+$, the decrease in peak boron concentration is smaller (from $1.2 \times 10^{19}$ to $7.3 \times 10^{18}\,cm^{-3}$) and the out-diffusion of the boron profile into the adjacent silicon layers is dramatically reduced. The boron profile of the $P^+$ and $F^+$ implanted sample shows less diffusion than seen in the unimplanted sample. Comparing the distance diffused by the boron in the SiGe (substrate side of the boron peak) at a concentration of $2 \times 10^{18}\,cm^{-3}$, we find a 58% decrease in the boron thermal diffusion in SiGe in the $P^+$ and $F^+$ implanted sample compared with the unimplanted sample (3 nm compared with 7.2 nm). This indicates that the $F^+$ implant in the latter sample has not only completely eliminated boron TED resulting from the $P^+$ implant, but has also significantly reduced boron thermal diffusion.

Fig. 4(a) compares the as-implanted fluorine profile with the annealed fluorine and boron profiles of the $P^+$ and $F^+$ implanted silicon sample. The annealed fluorine profile is considerably different than the as-implanted profile and shows two broad peaks. The deep peak lies within a depth range of 0.29–0.73 μm with a peak concentration of $8.31 \times 10^{19}\,cm^{-3}$ at a depth of 0.42 μm, which coincides with the as-implanted peak concentration

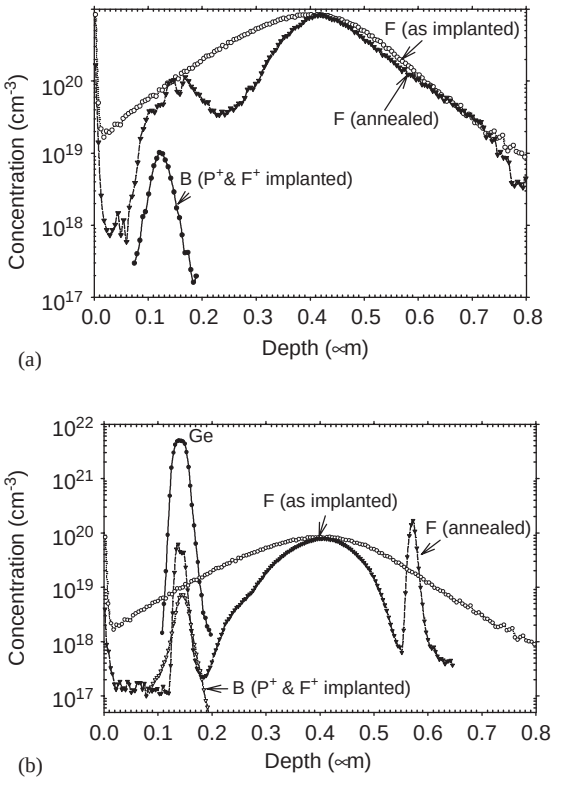



Fig. 4. Fluorine SIMS profiles before and after an anneal of 30 s at 1000 °C in dry $N_2$. Boron and germanium profiles after anneal are also included for reference. Results are shown for (a) a silicon sample and (b) a silicon germanium sample.

of $8.32 \times 10^{19}\,cm^{-3}$ at a depth of 0.42 μm. The shallow fluorine peak lies between 0.05 and 0.22 μm, and coincides with the boron profile. Four small peaks can be seen on the shallow fluorine peak at depths of 0.11, 0.12, 0.15 and 0.17 μm. The integrated dose of the as-implanted fluorine SIMS profile is $2.3 \times 10^{15}\,cm^{-2}$ and the integrated fluorine dose after anneal is $1.5 \times 10^{15}\,cm^{-2}$, indicating that 35% of the implanted fluorine has been lost during annealing. The majority of the fluorine lost comes from the surface side of the fluorine peak, but there is also some loss of fluorine from the substrate side.

Fig. 4(b) compares the as-implanted and annealed fluorine profiles of the $P^+$ and $F^+$ implanted SiGe sample. The germanium and boron profiles of the $P^+$ and $F^+$ implanted SiGe sample are also included for reference. The annealed fluorine profile is considerably different than the as-implanted profile and shows three distinct peaks. A deep sharp and narrow peak can be seen at a depth of 0.57 μm and coincides with the growth interface. A deep broad peak can be seen, which lies within a depth range of 0.28–0.55 μm with a peak concentration of $7.97 \times 10^{19}\,cm^{-3}$ at a depth of 0.41 μm. This peak concentration almost coincides with the as-implanted peak concentration of $8.32 \times 10^{19}\,cm^{-3}$ at a depth of 0.42 μm. A sharp and narrow shallow peak, which lies within the germanium profile between 0.12 and 0.17 μm can also bee seen. This peak shows two small peaks within it at depths of 0.14 and 0.15 μm, respectively. The integrated dose of the as-implanted fluorine SIMS profile is $2.3 \times 10^{15}\,cm^{-2}$ and the integrated fluorine dose after anneal is $1.5 \times 10^{15}\,cm^{-2}$, indicating that 35% of the implanted fluorine has been lost during annealing.

Fig. 5(a) shows cross-sectional transmission electron microscope micrographs of the $P^+$ and $F^+$ implanted silicon sample annealed at 1000 °C. The region from the

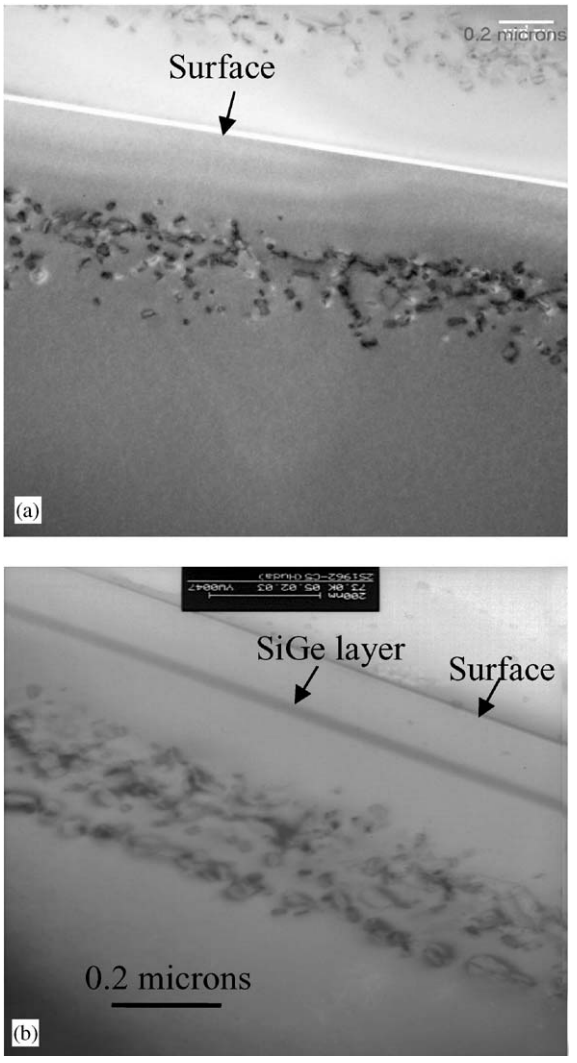



Fig. 5. Cross section transmission electron micrographs of $P^+$ and $F^+$ implanted samples annealed for 30 s at 1000 °C in dry $N_2$. Results are shown for (a) a silicon sample and (b) a silicon germanium sample.

surface to a depth of 0.29 μm is smooth with no visible defects. A band of high-density dislocation loops with various sizes is seen from a depth of 0.29 μm to a depth of 0.73 μm. There are no visible defects beyond 0.73 μm.

Fig. 5(b) shows the cross-sectional transmission electron microscope micrograph of the $P^+$ and $F^+$ implanted SiGe sample annealed at 1000 °C. The silicon cap and the silicon germanium layers appear smooth and defect free, indicating good crystalline quality and no relaxation within the silicon germanium layer. A band of high-density dislocation loops is seen in the epitaxial silicon layer from a depth of 0.29 μm to a depth of 0.66 μm. There are no visible defects beyond 0.66 μm.

Fig. 6 shows detailed cross sectional transmission electron microscope micrographs of the defects observed in the (a) $P^+$ and $F^+$ implanted silicon sample and (b) silicon germanium sample. The defects observed are similar in both samples and consist mainly of dislocation loops with varying shapes and sizes ranging from 11 to 96 nm.

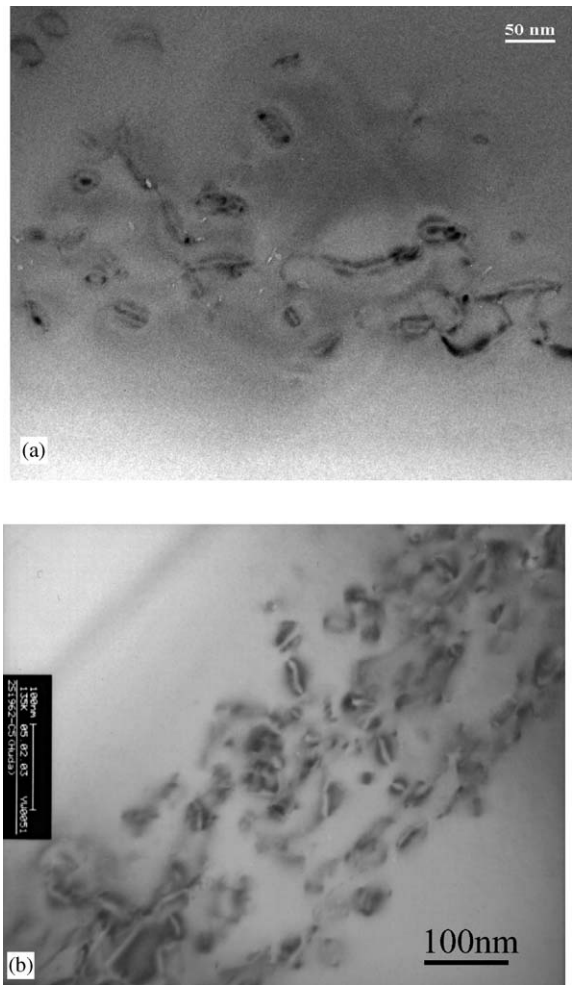



Fig. 6. High-resolution cross section transmission electron micrographs of $P^+$ and $F^+$ implanted samples annealed for 30 s at 1000 °C in dry $N_2$. Results are shown for (a) a silicon sample and (b) a silicon germanium sample.

## 4. Discussion

The results in Fig. 3(a) and (b) show that the high-energy $F^+$ implant has not only completely eliminated boron transient enhanced diffusion, but has also given a substantial 55% and 58% reduction in the thermal diffusion of boron in silicon and silicon germanium respectively.

A comparison of the SIMS profiles in Fig. 4(a) and (b) with the TEM micrographs in Fig. 5(a) and (b), shows that the deep fluorine peaks correlate with the band of dislocation loops observed. The deep fluorine peak in Fig. 4(a) extends from about 0.28 to 0.70 μm, which compares with the band of defects in Fig. 5(a) extending from about 0.29 to 0.73 μm. Similarly the deep fluorine peak in Fig. 4(b) extends from about 0.28 to 0.55 μm, which compares with the band of defects in Fig. 5(b) extending from about 0.29 to 0.66 μm. TEM micrographs of as-implanted layers (not presented) show that the phosphorus and fluorine implants did not amorphise the layers, hence, these defects are typical of the type of dislocation loops that result from sub-amorphising implants. Similar dislocation loops have been reported by Wu et al. [24] for a 49 keV, $2\times10^{15}\,cm^{-2}$ $BF_2^+$ implant after anneal at 900 °C for 30 min. The loops were reported to be perfect and faulted partial interstitial loops, with sizes ranging from ≈20–80 nm [24]. Similar dislocation loops resulting from a 0.5 MeV, $5\times10^{15}\,cm^{-2}$ $F^+$ implant into silicon and an anneal of 700 °C for 2 h, which correlated with a fluorine peak in the SIMS profile were reported [25]. Given the similarity between these reported loops and those in Figs. 5 and 6, and the location of the deep fluorine peak in the interstitial-rich region of the fluorine and phosphorus implants damage profiles [26], we suggest that the deep fluorine peak is due to fluorine trapping at interstitial dislocation loops.

The shallow fluorine peaks in Fig. 4 lie at a depth of about 0.07–0.22 μm, which corresponds to 0.17–0.53$R_p$, where $R_p$ is the range of the fluorine implant. Simulations of vacancy and interstitial profiles after implantation [26,27] have predicted a vacancy-rich region extending from the surface to a depth approaching the implantation range, $R_p$, and a deeper interstitial-rich region peaking at a depth just beyond $R_p$. This indicates that the shallow fluorine peaks lies in the vacancy-rich region of the damage profile. Work on the diffusion of fluorine in silicon has shown that fluorine diffuses extremely rapidly in silicon [28]. Thus on the basis of diffusion alone we would not expect to see much fluorine

remaining after the 30 s anneal at 1000 °C used in our work. The presence of large fluorine peaks in Fig. 3 after anneal, therefore, suggests that fluorine has been trapped at defects created by the fluorine implant. The TEM micrographs in Fig. 5 shows no evidence of extended defects down to a depth of 0.29 μm, and hence the trapping of fluorine at the shallow fluorine peaks in both silicon and silicon germanium must be due to defects that are too small to resolve by TEM.

There is considerable evidence in the literature for the formation of vacancy-fluorine clusters [13,17,25,28,29] that are too small to resolve by TEM. For example, Shano et al. [13] reported that boron diffusion was suppressed due to a fluorine peak in the vicinity of the boron, which was attributed to the presence of the $F–V_6$ cluster on the basis of ab initio calculations. Fluorine has been reported to diffuse towards the vacancy-rich surface region [25,28] due to its affinity for vacancies where it forms stable $F–V_3$ vacancy complexes, which result in suppression of boron transient enhanced diffusion [17,29]. Evidence of fluorine vacancy complexes close to the surface using positron annihilation spectroscopy has also been reported [25]. A similar shallow fluorine peak, formed after a 160 keV, $5 \times 10^{15}\,cm^{-2}$ $F^+$ implant and an anneal at 950 °C for 30 s, has also been reported in the literature and was attributed to the formation of F-filled bubbles [12]. Our results are consistent with the above work as we see a shallow fluorine peak in the vacancy-rich region close to the surface, which is not related to extended damage. This suggests that the shallow fluorine peak is due to the trapping of fluorine at vacancy-fluorine clusters.

Several alternative mechanisms have been proposed to explain the effect of fluorine in suppressing the transient enhanced diffusion of boron, including a chemical interaction between boron and fluorine [4,9,11,14,16] the presence of vacancy-fluorine clusters [13,17,18, 29] and the interaction of fluorine with interstitials [2,4–10,18]. In the present work, if the shallow fluorine peak was due to vacancy-fluorine clusters, as discussed above, we would expect that the clusters would give an under saturation of the local interstitial concentration, since any interstitials in the vicinity may be able to recombine and annihilate with vacancies at or near the vacancy–fluorine clusters. Since boron diffusion in silicon and silicon germanium is mediated by interstitials, an under-saturation of the interstitial concentration could give rise to a suppression of boron thermal diffusion. Alternatively, if the deep fluorine peak was due to trapping of fluorine at interstitial-type dislocation loops, this may prevent the release of interstitials and their back-flow to the surface. Such a mechanism could explain the suppression of boron transient enhanced diffusion by the fluorine. Further work is needed to verify these possibilities.

A comparison of the fluorine profile in SiGe shown in Fig. 4(b) with that in silicon shown in Fig. 4(a) shows that the two profiles are very different. The fluorine peak in the SiGe layer is very sharp and reaches concentrations that are much higher than the as-implanted concentrations at the equivalent depths. In contrast the fluorine peak in the silicon sample in the vicinity of the boron marker layer is very broad and at no point does the fluorine concentration exceed the as-implanted concentration. Furthermore, Fig. 4(b) shows that the fluorine concentration in the silicon layers immediately adjacent to the SiGe layer is very low. This indicates that the fluorine is transported from the silicon into the SiGe layer during anneal and that this effect is strong enough to give dramatically higher fluorine concentrations in the SiGe layer than in the adjacent silicon layers. This result could be explained if the vacancy–fluorine clusters formed more easily in SiGe than in Si.

## 5. Conclusions

In conclusion, a study has been made of the effect of a $F^+$ implant on boron diffusion in Si and SiGe. In samples implanted with $P^+$ and $F^+$, the fluorine not only completely suppresses boron transient enhanced diffusion in both Si and SiGe, but also significantly reduces boron thermal diffusion. Fluorine SIMS profiles show a broad deep fluorine peak almost coinciding with the implant range and a shallow fluorine peak in the vicinity of the boron profile. TEM observations show a band of dislocation loops, which correlate with the deep fluorine peak, but no defects are visible in the position of the shallow fluorine peak. It is proposed that the shallow fluorine peak is due to vacancy–fluorine clusters that are too small to resolve by TEM and that these clusters play a role in the suppression of boron thermal diffusion. The dislocation loops lie in the interstitial-rich region of the fluorine damage profile. It is proposed that the trapping of fluorine at these dislocation loops could play a role in trapping interstitials and thereby suppressing boron transient enhanced diffusion.

## Acknowledgement

The authors would like to acknowledge the Engineering and Physical Sciences Research Council for funding this work.

## References

[1] Wilson RG. Boron, fluorine and carrier profiles for B and $BF_2$ implants into crystalline and amorphous Si. J Appl Phys 1983;54(12):6879–89.

[2] Ohyu K, Itoga T, Natsuaki N. Advantages of fluorine introduction in boron implanted shallow p+/n junction formation. Jpn J Appl Phys 1990;29:457–62.
[3] Fan D, Parks JM, Jaccodine RJ. Effect of fluorine on the diffusion of through-oxide implanted boron in silicon. Appl Phys Lett 1991;59(10):1212–4.
[4] Krasnobaev LY, Omelyanovskaya NM, Makarov VV. The effect of fluorine on the redistribution of boron in ion implanted silicon. J Appl Phys 1993;74(10):6020–2.
[5] Huang TH, Kinoshita H, Kwong DL. Influence of fluorine preamorphization on the diffusion and activation of low energy implanted boron during rapid thermal annealing. Appl Phys Lett 1994;65(14):1829–31.
[6] Vuong H-H, Gossmann H-J, Rafferty CS, Luftman HS, Unterwald FC, Jacobson DC, Ahrens RE, Boone T, Zeitzoff PM. Influence of fluorine implant on boron diffusion: determination of process modelling parameters. J Appl Phys 1995;77(7):3056–60.
[7] Downey DF, Chow JW, Ishida E, Jones KS. Effect of fluorine on the diffusion of boron in ion implanted silicon. App Phys Lett 1998;73(9):1263–5.
[8] Park Y-J, Kim J-J. Fluorine implantation effect on boron diffusion in Si. J Appl Phys 1999;85(2):803–6.
[9] Liu J, Downey DF, Jones KS, Ishida E. Fluorine effect on boron diffusion : chemical or damage? Proceedings international conference ion implantation technology, vol. 2; 1999, p. 951–4.
[10] Ishida E, Downey DF, Jones KS, Liu J. The chemical effect of fluorine on boron transient enhanced diffusion. Proceedings international conference ion implantation technology. vol. 2; 1999, p. 909–12.
[11] Robertson LS, Warnes PN, Jones KS, Earles SK, Law ME, Downey DF, Falk S, Liu J. Junction depth reduction of ion implanted boron in silicon through fluorine ion implantation. Mater Res Soc Symp Proc 2000;610: B4.2.1–6.
[12] Ohno N, Hara T, Matsunaga Y, Current MI, Inoue M. Diffusion of ion implanted boron impurities into pre-amorphised silicon. Mater Sci Semicond Process 2000; 3:221–5.
[13] Shano TS, Kim R, Hirose T, Furuta Y, Tsuji H, Furuhashi M, Taniguchi K. Realization of ultra-shallow junction: suppressed boron diffusion and activation by optimised fluorine co-implantation. Technical Digest International Electron Devices Meeting; 2001. p. 37.4.1-4.
[14] Mokhberi A, Kasnavi R, Griffin PB, Plummer JD. Fluorine interaction with point defects, boron and arsenic in ion implanted Si. Appl Phys Lett 2002;80(19):3530–2.
[15] Jacques JM, Robertson LS, Jones KS, Bennett J, Rendon M. Effect of fluorine on the diffusion of boron in amorphous silicon. Mater Res Soc Symp Proc 2002;717:C4.6.1–6.
[16] Dusch A, Marcon J, Masmoudi K, Ketata K, Olivie F, Benzohra M, Ketata M. Influence of fluorine on the simulation of the transient enhanced diffusion of 15 keV $BF_2^+$ ion implantation into silicon. Nucl Instrum Methods Phys Res B 2002;186:360–5.
[17] Diebel M, Chakravarthi S, Machala CF, Ekbote S, Jain A, Dunham ST. Investigation and modelling of fluorine co-implantation effects on dopant redistribution. Mater Res Soc Symp Proc 2003;765:D6.15.1–6.
[18] El Mubarek HAW, Ashburn P. Reduction of boron thermal diffusion and elimination of boron transient enhanced diffusion in silicon by high energy fluorine implantation. Appl Phys Lett 2003;83(20):4134–6.
[19] Liu K, Wu J, Chen J, Jain A. Fluorine assisted super-halo for sub-50 nm transistors. IEEE Electron Dev Lett 2003;24:180–2.
[20] Fukutome H, Momiyama Y, Nakao H, Aoyama T, Arimoto H. Fluorine implantation impact in extension region on the electrical performance of sub-50 nm PMOS-FETS Technical Digest International Electron Devices Meeting, 2003. p. 485.
[21] Ashburn P. Design and realization of bipolar transistors. New York: Wiley; 1988.
[22] Eaglesham DJ, Stolk PA, Gossmann H-J, Poate JM. Implantation and transient B diffusion in Si: the source of the interstitials. Appl Phys Lett 1994;65(18):2305–7.
[23] Martinet B, Baudry H, Kermarrec O, Campidelli Y, Laurens M, Marty M, Schwartzmann T, Monroy A, Bensahel D, Chantre A. 100 GHz SiGe: C HBTs using non selective base epitaxy. Proceedings of the 31st European solid state device research conference; 2001. p. 97–100.
[24] Wu I-W, Fulks RT, Mikkelsen Jr JC. Optimization of $BF_2^+$ implanted and rapidly annealed junctions in silicon. J Appl Phys 1986;60(7):2422–38.
[25] Pi X D, Burrows CP, Coleman PG. Fluorine in silicon: diffusion, trapping and precipitation. Phys Rev Lett 2003;90 155901-1–4.
[26] Giles MD. Transient phosphorus diffusion below the amorphization threshold. J Electrochem Soc 1991;138: 1160–5.
[27] Sultan A, Banerjee S, List S, McNeil V. An approach using a subamorphizing threshold dose silicon implant of optimal energy to achieve shallower junctions. J Appl Phys 1998;83(12):8046–50.
[28] Robinson RR, Law ME. Fluorine diffusion: models and experiments. Technical Digest International Electron Devices Meeting, 2002. pp. 883–886.
[29] Diebel M, Dunham ST. Ab-initio calculations to model anomalous fluorine behavior. Mater Res Soc Sympo Proc 2002;717:C4.5.1–6.